2008 IEEE International Conference on
Robotics and Automation
Pasadena, CA, USA, May 19-23, 2008

Experimental comparison of several posture estimation solutions for biped robot *Rabbit*

Y. Aoustin, F. Plestan, V. Lebastard

Abstract— **Experimental validation of absolute orientation estimation solutions is displayed for the dynamical stable five-link biped robot *Rabbit* during a walking gait. The objective is to prove the technical feasibility of posture online software estimation in order to remove sensors. Finally, this paper presents the *first experimental results* of walking biped robot posture estimation.**

I. Introduction

Walking biped robots belong to the family of robots which use their environment to move and to accomplish their tasks. For this reason, the knowledge of several variable (positions in the environment, altitude of the swing leg tip) is crucial in order to predict and to control their motions. This problem is not trivial and is usually solved using sensors such as accelerometers, gyrometers, inertials units ... (for details, see [5], [16], [18], [24], [30]). In order to limit conception/maintenance costs, and to remove technological features such as noise, bandwidth limits of the sensor w.r.t. dynamics of the walking biped, an exciting challenge consists in using alternative solutions such as observers to estimate the orientation of the walking biped robot in imbalance phases. The dynamical behavior of a biped robot is described by a nonlinear model which implies that observability property depends on state and input [13], [17], [28]. A consequence is that, over one step, by supposing that only articular positions are measured, and for given trajectories, observability feature can be lost [22]. In this latter reference, an original strategy has been proposed in order to "cross" this singularity by using two observers based on different structures, each structure having different observability singular points.

Many observers strategies have been proposed for nonlinear systems. In [11], [32], observers based on linearization by input-output injection have been proposed: this approach consists in transforming the nonlinear system into a linear one via a state coordinates transformation and an input-output injection and in designing a classical Luenberger observer for this linear system. Unfortunately, this kind of observers can be applied only to a small subset of systems. In [10], high gain observers with an asymptotic convergence are proposed: their design is based on a canonical form [19] and concerns a large class of systems. In [14], [15], [25], [27], observers based on sliding mode are proposed with the objective to get robust estimation and finite time convergence. However, the main drawback of sliding mode being the "chattering" (high frequency oscillation), observers based on high order sliding mode (which ensures better features on robustness and accuracy by decreasing the chattering) have been proposed by [3], [7]. As high gain observers, this latter class of observers can be applied to a large class of physical systems including biped robots. However, to authors' best knowledge, previous works on observers design for biped robots have been mainly done for velocities estimation (in order to noiseless differentiation) by supposing that all angular variables are available [12], [26], [31]. The originality of authors' previous works consists in designing posture and velocities observers which is a hard but more realistic (by a practical point-of-view) task. In [21], [22], the estimation of posture during imbalance phases for three-link/five-link biped robots has been done in simulation by using high gain observers (with asymptotical time convergence) and high order sliding mode observers (with finite time convergence). Furthermore, the proof of the walking gait stability of the biped under an observer-based control has been established in [22].

The main purpose of the current paper consists in evaluating the behavior of different observers on the biped robot experimental platform *Rabbit* [6]. Previously, the absolute orientation of the experimental platform *SemiQuad* has been successfully estimated by using an extended Kalman filter [2]. However, *SemiQuad* has no available orientation measurement. Then, it was only possible to analyze the quality of this estimation at the end of the single support and at the beginning of the double support, by comparing the estimated posture with the posture given by the joint measurements results and the geometrical model of *SemiQuad*. This is not the case of *Rabbit*, viewed that it is equipped by an absolute encoder to measure its torso orientation (see Figure 2). In the current paper, experimental results of the application of nonlinear observers are displayed, through the comparison of the posture estimation and its real value given by an encoder. Note that *the main contribution and originality of this paper consist in presenting the first experimental results of posture estimation of a walking biped robot*: to authors' best knowledge, this kind of experimentations has never been previously done. From [1], [29], desired motions are given, and a *PID* controller with a friction compensation is locally implemented on each actuated joint. Only the measurements of the joint variables and the torques are injected in the observers.

The paper is organized as follows: technological details on *Rabbit* are recalled in Section II. The dynamic 2D model of

The authors are with IRCCyN, UMR 6597, CNRS, École Centrale de Nantes, Université de Nantes, France Yannick.Aoustin@irccyn.ec-nantes.fr

This work is supported by the National Agency of Research (ANR) via the Project of *PHEMA*

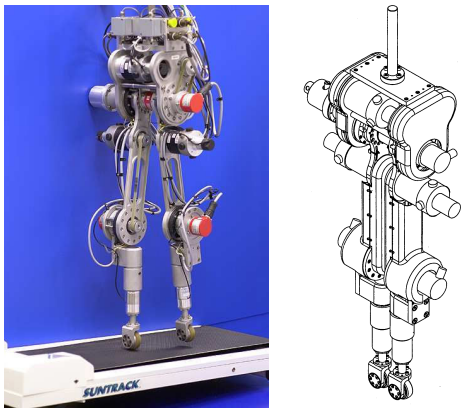

Fig. 1. **Left.** Photo of 5-link biped robot *Rabbit*. **Right.** *Rabbit*'s mechanical structure scheme.

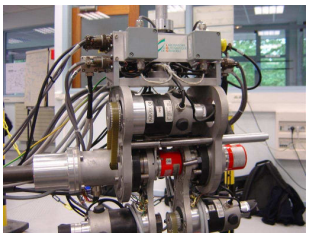

Fig. 2. Details of *Rabbit*'s hips, equipped with encoders.

Rabbit during a single support is presented in Section III. Section IV gives some details on the planning motion and the *PID* controller. Section V displays the three designed observers. Experimental results are shown in Section VI. Section VII contains our conclusion and perspectives.

II. Description of Rabbit

The *Rabbit* testbed was conceived to be the simplest mechanical structure still representative of human walking and running (Figure 1). It is composed of a torso and two identical double-link legs with knees. The legs have no feet. *Rabbit* walks in a circle and its motion is restricted to the sagittal plane with lateral stabilization: then, only 2D motion in the sagittal plane is considered. There are four electrical DC motors with gearbox reducers to actuate the hip joints (between the platform and the thighs) and the knee joints. To minimize the inertia of both legs, the actuators are located in the torso (Figure 2). The parameters of the five-links biped prototype "Rabbit" [6] are used to design the observers. The masses and lengths of the links (Indices 31, 41, 32, 42, 1: swing leg (femur, tibia), stance leg (femur, tibia), torso, resp.) are $m_{31} = m_{32} = 3.2\,kg$, $m_{41} = m_{42} = 6.8\,kg$, $m_1 = 17.0528\,kg$, $l_{31} = l_{32} = l_{41} = l_{42} = 0.4\,m$, $l_1 = 0.625\,m$. The distances between the joint and the mass center of each link are $s_{31} = s_{32} = 0.127\,m$, $s_{41} = s_{42} = 0.163\,m$, $s_1 = 0.1434\,m$. The inertia moments around the mass center of each link are $I_{31} = I_{32} = 0.0484\,kg{\cdot}m^2$, $I_{41} = I_{42} = 0.0693\,kg{\cdot}m^2$, $I_1 = 1.8694\,kg{\cdot}m^2$. The inertia of the rotor for each DC motor is $I = 3.32\,10^{-4}\,kg{\cdot}m^2$.

Friction effects in actuated joints are estimated with Coulomb coefficient $f_s = 18\ N.m$ and Kinematic coefficient $f_v = 8\ N.m/s$. The maximal value of the torque in the output shaft of each motor gearbox is $150\ N \cdot m$. The total mass of the biped is 37 kg approximately. Each actuated joint is equipped with two encoders measuring angular position. The first encoder, which has 250 $counts/rev$, is attached directly to the motor shaft, while the second, an absolute encoder which has 8192 $count/rev$, is attached to the shaft of the gear-reducer. This configuration allows any compliance between the motor and the joint angle to be detected. The angular velocities are calculated, using the angular positions given by the encoder attached directly to the motor shaft. An encoder measures the angle of the torso with respect to a vertical axis established by the central column around which *Rabbit* walks. In the sequel of the paper, this latter measurement is compared to the estimated torso orientation. In the case of *Rabbit*, one has approximately a 16 Hz bandwidth in the joints mechanical part and approximately 1.7 kHz for the amplifiers. The contact between the leg tip and the ground is detected with a contact switch.
In order to get measurement data and to implement the control algorithm, a *dSPACE* system has been selected as real-time control platform. The low-level computation, digital-to-analog and analog-to-digital conversion, as well as the user interface are provided by the *dSPACE* package. The control computations are performed with a sampling period of 1.5 ms (667 Hz).

III. Model of a planar five-link biped robot

In the sequel, observers are tested with data recorded during a single support phase of *Rabbit*'s experimental walking gait. For this reason, only the dynamic model of the single support phase in the sagittal plane of *Rabbit* is presented in this section. The considered biped is walking on a rigid and horizontal surface. *Rabbit* is modeled as a planar biped with a torso and two legs with knees but no actuated ankles (Figure 3). The walking cycle takes place in the sagittal plane and consists of successive single support phases and impact events. The complete model of the biped robot consists of two parts: differential equations describing dynamics of the robot during the swing phase, and an impulse model of the contact event [29]. The dynamic model of the biped in single support phase between successive impacts is derived from the Lagrange formalism

$$D(q_{rel})\ddot{q} + H(q,\dot{q})\dot{q} + G(q) + F(\dot{q}_{rel}) \quad = \quad B\Gamma \qquad (1)$$

with $q = [q_{31}\ q_{41}\ q_{32}\ q_{42}\ q_1]^T$, $q_{rel} := [q_{31}\ q_{32}\ q_{41}\ q_{42}]^T$, the vector joint angles vector, $\Gamma = [\Gamma_1\ \Gamma_2\ \Gamma_3\ \Gamma_4]^T$ (see Figure 3) the control torques [1], D the inertia matrix, H the centrifugal and Coriolis effects matrix and G the vector tacking into account the gravity effects. For the design of observers a friction term $F(\dot{q}_{rel})$ are considered in the actuated joint with the Coulomb coefficient f_s and Kinematic coefficient f_v defined in Section II. The torques Γ are applied between the torso and the stance leg, the torso and the swing leg, at

[1]Leg 1 is the stance one, leg 2 the swing one.

the knee of the stance leg, and at the knee of the swing leg, respectively. Then, the model can be written in state space form by defining

$$\begin{aligned} \dot{x} &= \begin{bmatrix} \dot{q} \\ D^{-1}(-H\dot{q} - G - F(\dot{q}_{rel}) + B\Gamma) \end{bmatrix} \\ &= f(x) + g(q_{rel}) \cdot \Gamma \end{aligned} \tag{2}$$

with $x = [q^T \ \dot{q}^T]^T$, where $q = [q_{31},\ q_{32},\ q_{41},\ q_{42},\ q_1]$. The state space is taken such that $x \in \mathcal{X} \subset I\!R^{10} = \{x = [q^T \ \dot{q}^T]^T \mid \dot{q} \in \mathcal{N},\ q \in \mathcal{M}\}$, where $\mathcal{N} = \{\dot{q} \in I\!R^5 \mid |\dot{q}| < \dot{q}_M < \infty\}$ and $\mathcal{M} = (-\pi, \pi)^5$. The walking surface is taken as $x \in \mathcal{S} = \{x \in \mathcal{X} \mid z_2(q) = 0,\ \dot{z}_2(q) < 0\}$ with $z_2(q)$ the altitude of the swing leg tip and its time derivative $\dot{z}_2(q)$. Note that input term of system (2), $g(q_{rel}) \cdot \Gamma$, depends

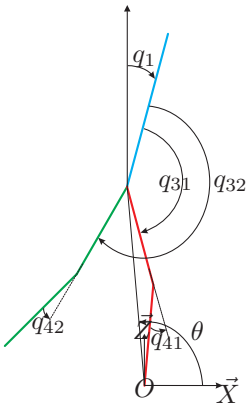

Fig. 3. Schematic of biped robot: absolute and relative angles.

on available data only, *i.e.* control input and measurements. This property allows to simplify the synthesis of observers through a more simple canonical form as it has been detailed in [21].

IV. Controller

The planning motion is based on the virtual constraints [1], [6], [29] using the absolute orientation θ of the virtual stance leg (Figure 3) to define the polynomial functions of the reference trajectory for the actuated joint variables. The coefficients of each polynomial functions have been obtained by optimization [8]. The control law is a *PID* controller associated to a friction compensation [4], [31].

V. Observers design

This section is divided in two parts: the first one consists in analyzing the observability of system (2), which has consequences on the observation strategy. The second part displays the three observation algorithms implemented on *Rabbit*.

A. Observability analysis

Consider system (2) with y the vector composed of the measured variables $y := [y_1 \ y_2 \ y_3 \ y_4]^T = [q_{31} \ q_{32} \ q_{41} \ q_{42}]^T = q_{rel}$

$$\begin{aligned} \dot{x} &= f(x) + g(y)\Gamma \\ y &= [I_{4\times4} \ \ 0_{4\times6}]\, x = Cx \end{aligned} \tag{3}$$

Observers are designed in the sequel for this latter system. Let $\mathcal{T}$ denote an open set of $\mathcal{X}$ such that the condition of the following definition is fulfilled.

Definition 1: System (3) is observable if there exist $\mathcal{T} \subset \mathcal{X}$ and 4 integers $\{k_1, k_2, k_3, k_4\}$, called *observability indexes*, such that $\sum_{i=1}^{4} k_i = 10$ and the transformation $\left[y_1 \ \cdots \ y_1^{(k_1-1)} \ \cdots \ y_4 \ \cdots \ y_4^{(k_4-1)}\right]^T = \Phi(x)$ is a diffeomorphism for $x \in \mathcal{T}$, which is equivalent to

$$\mathrm{Det}\left[\frac{\partial \Phi(x)}{\partial x}\right] \neq 0 \quad \text{for } x \in \mathcal{T}.$$

■

Proposition 1 ([21]): There exist $\mathcal{T} \subset \mathcal{X}$ and observability indexes vector $[k_1 \ k_2 \ k_3 \ k_4]^T$ such that system (3) is observable for $x \in \mathcal{T}$. ■

Suppose that Proposition 1 is fulfilled; then, the following associated state coordinates transformation is invertible

$$z = \Phi(x) = \left[y_1 \ \cdots \ y_1^{(k_1-1)} \ \cdots \ y_4 \ \cdots \ y_4^{(k_4-1)}\right]^T \tag{4}$$

Under this state transformation (4), system (3) is equivalent to the canonical form,

$$\begin{aligned} \dot{z} &= Az + \varphi(z, \Gamma) \\ y &= Cz \end{aligned} \tag{5}$$

with $A = \mathrm{diag}\,[A_1 \ \cdots \ A_4]_{10\times10}$, $C = [C_1 \ \cdots \ C_4]^T_{4\times10}$, $\varphi(z) = [\varphi_1^T \ \cdots \ \varphi_4^T]^T$, A_i and C_i being under Brunovsky's form. Function $z = \Phi(x)$ is a diffeomorphism from $\mathcal{T}$ onto $\mathcal{Z} = \Phi(\mathcal{T}) \subset I\!R^{10}$. Let $z_i = [z_{i1} \cdots z_{ik_i}]^T := \left[y_i \cdots y_i^{(k_i-1)}\right]^T \in \mathcal{Z}_i \subset I\!R^{k_i}$. During the swing phase, along the *nominal* trajectories, for each observability indices possibilities, there is loss of observability (see Figure 4 for $[k_1 \ k_2 \ k_3 \ k_4]^T = [3\ 3\ 2\ 2]^T$: determinant of $\frac{\partial \Phi(x)}{\partial x}$ is crossing zero). Of course, it induces a problem for the observer design. A solution consists in designing observers for several combinations of observability indices, for which the observability singularity appears for different articular positions. As a matter of fact, $[k_1 \ k_2 \ k_3 \ k_4]^T = [3\ 2\ 2\ 3]^T$ is also eligible: the evolution for a half step of $\mathrm{Det}\left[\frac{\partial \Phi(x)}{\partial x}\right]$ is displayed in Figure 4 (dotted line). There is no clear physical explanation why this determinant crosses the abscissa 0. Then an intuitive solution has been proposed, which consists in designing, over one step, two observers based on two different observability indexes vectors trajectories. There is a switching in one chosen time between the two observers.

Observation algorithm [21]. During the swing phase, along the *nominal* trajectories, for each observability indices possibilities, there is loss of observability (see Figure 4 for $[k_1 \ k_2 \ k_3 \ k_4]^T = [3\ 3\ 2\ 2]^T$: determinant of

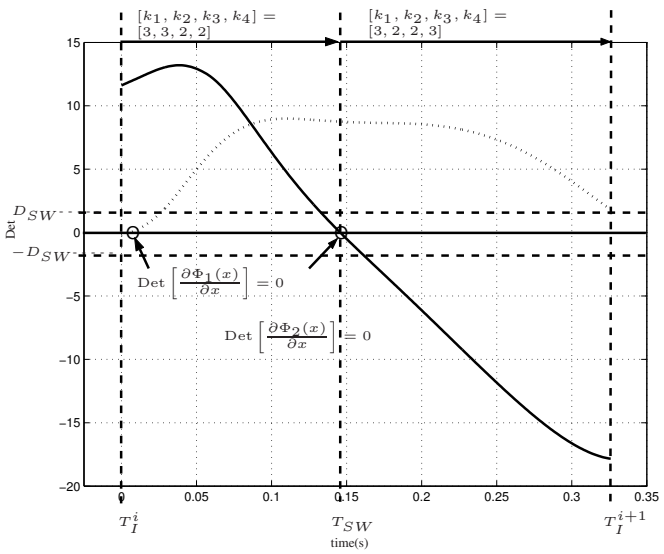

Fig. 4. Determinants of $\frac{\partial \Phi_1(\hat{x})}{\partial \hat{x}}$ (Bold line) and $\frac{\partial \Phi_2(\hat{x})}{\partial \hat{x}}$ (Dotted line) versus time (s.) over one step.

$\frac{\partial \Phi(x)}{\partial x}$ is crossing zero). Of course, it induces a problem for the observer design. A solution consists in designing observers for several combinations of observability indices, for which the observability singularity appears for different articular positions. As a matter of fact, $[k_1\ k_2\ k_3\ k_4]^T = [3\ 2\ 2\ 3]^T$ is also eligible: the variation of determinant of $\frac{\partial \Phi(x)}{\partial x}$ is displayed in Figure 4 (dotted line). Then, there exists $\mathcal{T}' \subset \mathcal{X}$ such that, $\forall x \in \mathcal{T}'$, the function $z = \Phi(x) = \left[\ y_1\ \dot{y}_1\ \ddot{y}_1\ y_2\ \dot{y}_2\ y_3\ \dot{y}_3\ y_4\ \dot{y}_4\ \ddot{y}_4\ \right]^T$ is a state transformation. Let $\mathcal{T}$ and $\mathcal{T}'$ defined such that

$$\begin{aligned}
\mathcal{T} &= \left\{ x \in \mathcal{X} \mid \mathrm{rank}\left[\frac{\partial \Phi_1}{\partial x}\right] = 10 \right\} \\
\Phi_1(x) &= \left[\ y_1\ \dot{y}_1\ \ddot{y}_1\ y_2\ \dot{y}_2\ \ddot{y}_2\ y_3\ \dot{y}_3\ y_4\ \dot{y}_4\ \right]^T \\
\mathcal{T}' &= \left\{ x \in \mathcal{X} \mid \mathrm{rank}\left[\frac{\partial \Phi_2}{\partial x}\right] = 10 \right\} \\
\Phi_2(x) &= \left[\ y_1\ \dot{y}_1\ \ddot{y}_1\ y_2\ \dot{y}_2\ y_3\ \dot{y}_3\ y_4\ \dot{y}_4\ \ddot{y}_4\ \right]^T
\end{aligned}$$

Note that Φ_1 (resp. Φ_2) corresponds to $[k_1\ k_2\ k_3\ k_4]^T = [3\ 3\ 2\ 2]^T$ (resp. $[k_1\ k_2\ k_3\ k_4]^T = [3\ 2\ 2\ 3]^T$). Define T_I^i (resp. T_I^{i+1}) the initial (resp. final) impact time of the step i. Let $T_{SW} := \mathrm{Min}(t)$ such that $t \in [T_I^i, T_I^{i+1}[$ and $\mathrm{Det}\left[\frac{\partial \Phi_1(x)}{\partial x}\right](t) = 0$).

Proposition 2 ([21]): An observer for system (3) can be written as

$$\dot{\hat{x}} = f(\hat{x}) + g(y)\Gamma + M(\hat{x}, y) \tag{6}$$

with

$$M = \begin{cases} \left[\frac{\partial \Phi_1(\hat{x})}{\partial \hat{x}}\right]^{-1} \gamma_1(\hat{x}, y) & \text{for} \quad t \in [T_I^i, T_{SW}[\\ \left[\frac{\partial \Phi_2(\hat{x})}{\partial \hat{x}}\right]^{-1} \gamma_2(\hat{x}, y) & \text{for} \quad t \in [T_{SW}, T_I^{i+1}[\end{cases}$$

where $\gamma_1(\cdot)$ and $\gamma_2(\cdot)$ are appropriate-dimensional correction matrices. ■

B. Observers design

In this part, three observers are displayed: high gain observer [10], step-by-step sliding mode observer [3], and observer based on high order sliding mode differentiation [7]. All these observers read as (6), their differences being in the definition of terms γ_1 and γ_2. Whereas high-gain observer ensures an asymptotic convergence of the estimation error, a feature of the both sliding mode ones is their finite time convergence; this latter point greatly simplifies the proof of stability [21].

High gain observer. Suppose that function φ of system (5) is globally Lipschitzian with respect to z. Then, system (5) is locally uniformly observable [9]. Let K denote a matrix of appropriate dimensions, such that $A - KC$ is Hurwitz, and $\Lambda(T) = \mathrm{diag}[\Lambda_1\ \Lambda_2\ \cdots\ \Lambda_p]'$ with $\Lambda_i = \mathrm{diag}[\tau_i\ \tau_i^2\ \cdots\ \tau_i^{k_i-1}]$, with $\tau_i > 0$. Then, the system

$$\dot{\hat{z}} = A\hat{z} + \varphi(\hat{z}) + \Lambda^{-1}K(y - C\hat{z}) \tag{7}$$

with $\hat{z} \in I\!R^n$, is an asymptotic observer for (5). Furthermore, the dynamics of this observer can be made arbitrarily fast. Then, with respect to system (6), matrices γ_1 and γ_2 read as (with adequate dimensions, symbol "*" being 1 or 2)

$$\gamma_* = \Lambda_*^{-1}K_*(y - C\hat{x})$$

Step-by-step sliding mode observer. The observer is based on triangular form one [3] and its main property is the finite time convergence to zero of the estimation error. System (5) is still on (particular) triangular form. A such observer of (5) can be written as [3]

$$\dot{\hat{z}} = A\hat{z} + \varphi(\hat{z}) + E(t)\chi(\cdot) \tag{8}$$

with $\hat{z} \in \mathcal{Z}$ the estimated vector of z. Knowing that the principle of this class of observers consists in forcing, each in turn, estimated state variables to corresponding real ones, in finite time, this latter property is based on an adequate choice of $E(t)$ and $\chi(\cdot)$, *i.e.* $E(t)$ and χ are defined such that the estimation error $e = \hat{z} - z$ converges to zero in finite time. The originality in the following is the use of the *super twisting algorithm* [23] in order to ensure the finite time algorithm: this allows to not use time derivative of estimation error in the computation of the observer.

Finite time convergence observer In a sake of clarity, and without loss of generality, only the observer design for a third order system is fully displayed in the sequel, *i.e.* $z \in \mathcal{Z} \in I\!R^3$. Then, in this case, system (5) reads as

$$\begin{aligned}
\dot{z}_1 &= z_2 \\
\dot{z}_2 &= z_3 \\
\dot{z}_3 &= f_3(z) \\
y &= z_1
\end{aligned} \tag{9}$$

with $z = [z_1\ z_2\ z_3]^T$. Then, an observer for (9) reads as

$$\begin{aligned}
\dot{\hat{z}}_1 &= \hat{z}_2 + E_1(t)\chi_1(\cdot) \\
\dot{\hat{z}}_2 &= \hat{z}_3 + E_2(t)\chi_2(\cdot) \\
\dot{\hat{z}}_3 &= f_3(\hat{z}) + E_3(t)\chi_3(\cdot)
\end{aligned} \tag{10}$$

with $E_i(t)$ and χ_i $(1 \leq i \leq 3)$ defined such that each estimation error $e_i = \hat{z}_i - z_i$ converges to zero. To ensure a finite time convergence, the function $\chi_i(\cdot)$ is based on the *super twisting algorithm* [23] and reads as

$$\chi_i = \varsigma_i + \lambda_i \ |S_i|^{1/2} \ \text{sign}(S_i), \ \dot{\varsigma}_i = \alpha_i \ \text{sign}(S_i) \qquad (11)$$

with

$$S_i \ = \ \begin{cases} y - Cz & \text{for} \quad i = 1 \\ \tilde{z}_i - \hat{z}_i & \text{for} \quad i > 1 \end{cases} \qquad (12)$$

and $\tilde{z}_j = \hat{z}_j + E_{j-1}(t)\chi_{j-1}$ for $j \in \{2, 3\}$.

Determination of E_i and sketch of proof of finite time convergence From (9)-(10), the dynamics of estimation error, $e_i = \hat{z}_i - z_i$, reads as

$$\begin{array}{l} \dot{e}_1 = e_2 + E_1(t)\chi_1(\cdot) \\ \dot{e}_2 = e_3 + E_2(t)\chi_2(\cdot) \\ \dot{e}_3 = f_3(\hat{z}) - f_3(z) + E_3(t)\chi_3(\cdot). \end{array} \qquad (13)$$

Step 1. Suppose that $e_1(0) \neq 0$, and observer (10) is initialized such that $E_1 = 1$ and $E_2 = E_3 = 0$. The error dynamics reads as

$$\dot{e}_1 = e_2 + \chi_1, \ \dot{e}_2 = e_3, \ \dot{e}_3 = f_3(\hat{z}) - f_3(z) \qquad (14)$$

As χ_1 is based on the *super twisting algorithm* with appropriate gain value, e_1 reaches zero in finite time at $t = t_1$. Then, $\forall \ t \geq t_1$, $e_1(t) = \dot{e}_1(t) = 0$, *i.e.*

$$e_1 = 0, \qquad \dot{e}_1 = e_2 + \chi_1 = \hat{z}_2 - z_2 + \chi_1 = 0 \qquad (15)$$

From (15), one gets $\hat{z}_2 + \chi_1 = z_2$ and $z_2 = \tilde{z}_2$.

Steps 2 and 3. The proof takes the same way than step 1.

Observer based on high order sliding mode differentiation. The observer proposed in the sequel is based on high order sliding mode differentiation. As previously, viewed that observability indexes equal 2 or 3, for a sake of clarity and without loss of generality, the observer design for a second (*i.e.* $k_i = 2$) order system and third (*i.e.* $k_i = 3$) is fully displayed in the sequel. Then, in the second order case, subsystem takes the form as [7]

$$\begin{array}{lcl} \dot{z}_{i1} & = & z_{i2} \\ \dot{z}_{i2} & = & \varphi_{ii}(z) \\ y_i & = & z_{i1} \end{array} \qquad (16)$$

with $\|\varphi_{ii}(\cdot)\| \leq L_{ii}^2$. Then, an observer for (16) reads as [7]

$$\begin{array}{lcl} \dot{\hat{z}}_{i1} & = & \hat{z}_{i2} + 1.5 \ L_{ii}^{1/2}|z_{i1} - \hat{z}_{i1}|^{1/2}\text{sign}(z_{i1} - \hat{z}_{i1}) \\ & = & v_{i1} \\ \dot{\hat{z}}_{i2} & = & \varphi_{i2}(\hat{z}_i) + 1.1 \ L_{ii}\text{sign}(v_{i1} - \hat{z}_{i1}) \end{array} \qquad (17)$$

with $[\hat{z}_{i1} \ \hat{z}_{i2}]^T$ the estimation of $[z_{i1} \ z_{i2}]^T$. In the third order case, subsystem reads as

$$\begin{array}{lcl} \dot{z}_{i1} & = & z_{i2} \\ \dot{z}_{i2} & = & z_{i3} \\ \dot{z}_{i3} & = & \varphi_{ii}(z) \\ y_i & = & z_{i1} \end{array} \qquad (18)$$

with $\|\varphi_{ii}(\cdot)\| \leq L_{ii}$. Let us propose an observer for the jerk observation based on a third order differentiator [20]

$$\begin{array}{lcl} \dot{\hat{z}}_{i1} & = & \hat{z}_{i2} + 2 \ L_{ii}^{1/3}|z_{i1} - \hat{z}_{i1}|^{2/3}\text{sign}(z_{i1} - \hat{z}_{i1}) \\ & = & v_{i1} \\ \dot{\hat{z}}_{i2} & = & \hat{z}_{i3} + 1.5 \ L_{ii}^{1/2}|v_{i1} - \hat{z}_{i2}|^{1/2}\text{sign}(v_{i1} - \hat{z}_{i2}) \\ & = & v_{i2} \\ \dot{\hat{z}}_{i3} & = & \varphi_{i3}(\hat{z}_i) + 1.1 \ L_{ii}\text{sign}(v_{i2} - \hat{z}_{i3}) \end{array} \qquad (19)$$

with $[\hat{z}_{i1} \ \hat{z}_{i2} \ \hat{z}_{i3}]^T$ the estimation of $[z_{i1} \ z_{i2} \ z_{i3}]^T$. Then, correction terms of observer (6), γ_1 and γ_2, are composed of correction terms of (17)-(19) written in x-state space coordinates.

VI. Experimental results

A walking gait of several steps has been made. All experimental data are recorded with a sampling period of $1.5 \ ms$. Only actuated joint positions (single measurements) and torques (control inputs) are injected in (6). For high gain observer, $A - KC$-eigenvalues equal -1 and -2. Its gains are such that $\tau_i = 0.3$, $i = 1, 2, 3, 4$. Considering the step-by-step sliding mode observer, for subsystems corresponding to observability indice equal to 2 (resp. 3), parameters are $\alpha_1 = \lambda_1 = 1$, $\alpha_2 = \lambda_2 = 4$ (resp. $\alpha_1 = \lambda_1 = 1$, $\alpha_2 = \lambda_2 = 4$, $\alpha_3 = \lambda_3 = 20$). For the observer based on high order sliding mode differentiation the gains are $L = 3$. In Figure 5, the orientation estimation error and its velocity are presented for the three observers from an impact (at the initial time) to the next impact (at the final time) (note that the robot is still walking with a stable periodic motion). The estimation error module for the angular value is less than 2 degrees at the end of the step. The estimation error module for its velocity is less than $0.65 \ rad.s^{-1}$. These results prove the practical feasibility of the proposed solution. Furthermore, robustness of the estimation has been evaluated through the following test: a mass of $5.0 \ kg$ has been added to the torso of *Rabbit* during the walking gait, without changing this parameter in the observers. For this kind of disturbance, Figure 6 shows that the three observers are not very sensitive viewed that the estimation error at the end of the step is still reasonable. Furthermore at the end with the swing leg-touch, in double support it is always possible to update the observer by calculating the orientation of the torso, using the geometrical model.

VII. Conclusion

In this paper, three nonlinear observers have been designed and experimentally tested on the biped robot *Rabbit*, in order to estimate its posture. The experimental results show that the orientation estimation is feasible and is a good alternative to sensors. Next step of this work consists, first, in associating a nonlinear dynamic control law (based on the model of *Rabbit*) with posture observers, in order to get stable walking gait. Secondly, impact effects could be taken into account in the observers design in order to improve their performances. Finally, a major perspective is to extend this strategy for walking 3D-biped robots.

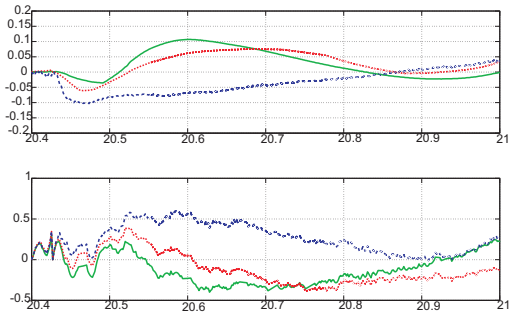

Fig. 5. **Top.** Estimation error of posture q_1 $(deg.)$ versus time (sec.) [Solid line: high gain observer - Dashed Line: step-by-step observer - Dotted line: differentiator based observer]. **Bottom.** Estimation error of velocity $\dot{q}_1$ $(rad.s^{-1})$ versus time (sec.)

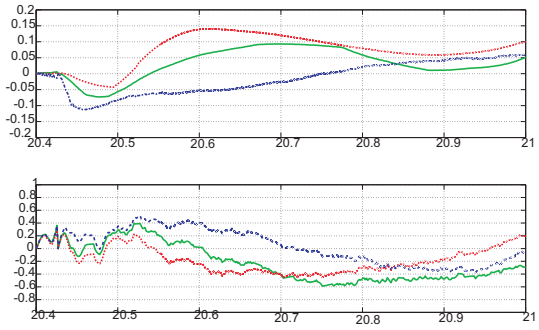

Fig. 6. Robustness evaluation. **Top.** Estimation error of posture q_1 $(deg.)$ versus time (sec.) [Solid line: high gain observer - Dashed Line: step-by-step observer - Dotted line: differentiator based observer]. **Bottom.** Estimation error of velocity $\dot{q}_1$ $(rad.s^{-1})$ versus time (sec.)

ACKNOWLEDGMENTS

The authors would like to greatly thank Gabriel Buche, from LAG (Grenoble, France), for his very helpful collaboration during all the experimentations.

REFERENCES

[1] Y. Aoustin and A.M. Formal'sky. Control design for a biped: reference trajectory based on driven angles as functions of the undriven angle. *International Journal of Computer and Systems Sciences*, 42(4):159–176, 2003.

[2] Y. Aoustin, G. Garcia, and Ph. Lemoine. *Biped estimation of the absolute orientation of a five-link walking robot with passive feet*. Humanoid Robots, Vienna, Austria, EU, 2007.

[3] T. Boukhobza and J.P. Barbot. High order sliding modes observer. In *Proc. IEEE Conf. on Decision and Control CDC*, Tampa, Florida, USA, 1998.

[4] C. Canudas de Wit, Artrom K. J., and K. Braun. Adaptative friction compensation in dc-motor drives. *IEEE International Journal of Robotics and Automation*, 3(6):681–685, 1987.

[5] N. Chaillet. *Etude et réalisation d'une commande position-force d'un robot bipède*. PhD thesis, Université Louis Pasteur de Strasbourg, 1993.

[6] C. Chevallereau, G. Abba, Y. Aoustin, F. Plestan, E.R. Westervelt, C. Canudas de Wit, and J.W. Grizzle. Rabbit: a testbed for advanced control theory. *IEEE Control Systems Magazine*, 23(5):57–79, 2003.

[7] J. Davila, L. Fridman, and A. Levant. Second-order sliding-mode observer for mechanical systems. *IEEE Transactions on Automatic Control*, 50(11):1785–1789, 2005.

[8] D. Djoudi. *Contribution à la commande d'un robot bipède*. PhD thesis, Ecole Centrale et Université de Nantes, 2007.

[9] J. P. Gauthier and G. Bornard. Observablity for any $u(t)$ of a class of nonlinear systems. *IEEE Transactions on Automatic Control*, 26(4):922–926, 1981.

[10] J.P. Gauthier, H. H.Hammouri, and S. Othman. A simple observer for nonlinear systems, application to bioreactors. *IEEE Transations on Automatic Control*, 37(6):875–880, 1992.

[11] A. Glumineau, C. Moog, and F. Plestan. New algebro-geometric conditions for the linearization by input-output injection. *IEEE Transactions on Automatic Control*, 41(4):598–603, 1996.

[12] J. W. Grizzle, J. H. Choi, H. Hammouri, and B. Morris. On observer-based feedback stabilization of periodic orbits in bipedal locomotion. In *Proc. Methods and Models in Automation and Robotics MMAR*, Szczecin, Poland, EU, 2007.

[13] R. Hermann and A. J. Krener. Nonlinear controllability and observability. *IEEE Transactions On Automatic Control*, 22(5):728–740, 1977.

[14] J. Hernandez and J. P. Barbot. Sliding observer based feedback control for exible joint manipulators. *Automatica*, 32(9):1243–1254, 1996.

[15] J. P. Hespanha, D. Liberzon, and E. D. Sontag. Nonlinear observability and an invariance principle for switched systems. In *Proc. IEEE Conf. on Decision and Control CDC*, Las-Vegas, Nevada, USA, 2002.

[16] K. Hirai, M. Hirose, and T. Haikawa. The development of honda humanoid robot. In *Proc. IEEE Conf. on Robotics and Automation ICRA*, Leuven, Belgium, 1998.

[17] A. Isidori. *Nonlinear Control Systems*. Springer-Verlag, London, England, 1995.

[18] K. Kaneko, F. Kanehiro, S. Kajita, H. Hirukawa, T. Kawasaki, M. Hirata, K. Akachi, and T. Isozumi. Humanoid robot hrp-2. In *Proc. IEEE Int. Conf. on Robotics and Automation ICRA*, New-Orleans, Louisiana, USA, 2004.

[19] H. Keller. Nonlinear observer design by transformation into a generalized observer canonical form. *International Journal of Control*, 46(6):1915–1930, 1987.

[20] V. Lebastard, Y. Aoustin, and F. Plestan. Absolute orientation estimation based on high order sliding mode observer for a five-link walking biped robot. In *Proc. 9th IEEE Workshop on Variable Structure Systems VSS'06*, Alghero, Italy, 2006.

[21] V. Lebastard, Y. Aoustin, and F. Plestan. *Lecture Notes in Control and Information Sciences*, volume 335 of *1-84628-404-X*, chapter Absolute orientation estimation for observer-based control of a five-link walking biped robot. Springer, 2006.

[22] V. Lebastard, Y. Aoustin, and F. Plestan. Observer-based control of a walking biped robot without orientation measurement. *Robotica*, 24(3):385–400, 2006.

[23] A. Levant. Sliding order and sliding accuracy in sliding mode control. *International Journal of Control*, 58(6):1247–1263, 1993.

[24] K. Löffler, M. Gienger, and F. Pfeiffer. Trajectory control of a biped robot. In *Proc. 5th International Conference on Climbing and Walking Robots*, Paris, France, 2002.

[25] V. Lòpez-M., F. Plestan, and A. Glumineau. An algorithm for the structural analysis of state space: synthesis of nonlinear observers. *International Journal of Robust and Nonlinear Control*, 11(12):1145–1160, 2001.

[26] P. Micheau, M.A. Roux, and P. Bourassa. Self-tuned trajectory control of a biped walking robot. In *Proc. Int. Conf. on Climbing and Walking Robot CLAWAR*, Catania, Italy, 2003.

[27] W. Perruquetti, T. Floquet, and P. Borne. A note on sliding observer and controller for generalized canonical form. In *Proc. IEEE Conf. on Control and Decision CDC*, Tampa, Florida, USA, 1998.

[28] F. Plestan and A. Glumineau. Linearization by generalized input-output injection. *Systems and Control Letters*, 31(2):115–128, 1997.

[29] F. Plestan, J.W. Grizzle, E.R. Westervelt, and G. Abba. Stable walking of a 7-dof biped robot. *IEEE Transactions on Robotics and Automation*, 19(4):653–668, 2003.

[30] P. Sardin, M. Rostami, E. Thomas, and G. Bessonnet. Biped robots: Correlation between technological design and dynamic behaviour. *Control Engineering Practice*, 7:401–411, 1999.

[31] E. R. Westervelt, G. Buche, and J. W. Grizzle. Experimental validation of a framework for the design of controllers that induce stable walking in planar bipeds. *The International Journal of Robotics Research*, 24(6):559–582, 2004.

[32] X. Xia and W. Gao. Nonlinear observer design by observer error linearization. *SIAM Journal of Control and Optimisation*, 27(1):199–213, 1989.